ISSN 0021-8944, Journal of Applied Mechanics and Technical Physics, 2023, Vol. 64, No. 1, pp. 98–109. © Pleiades Publishing, Ltd., 2023.
Russian Text © V.V. Vasiliev, S.A. Lurie.

DIFFERENTIAL EQUATIONS AND THE PROBLEM OF SINGULARITY OF SOLUTIONS IN APPLIED MECHANICS AND MATHEMATICS

V. V. Vasiliev[a,*] **and S. A. Lurie**[b]

UDC 501

Abstract: A modified form of differential equations is proposed that describes physical processes studied in applied mathematics and mechanics. It is noted that solutions to classical equations at singular points may undergo discontinuities of the first and second kind, which have no physical nature and are not experimentally observed. When new equations describing physical fields and processes are derived, elements with finite dimensions are considered instead of infinitely small elements of the medium. Thus, classical equations include nonlocal functions averaged over the element volume and are supplemented by the Helmholtz equations establishing a relationship between nonlocal and actual physical variables, which are smooth functions having no singular points. Singular problems of the theory of mathematical physics and the theory of elasticity are considered. The obtained solutions are compared with the experimental results.

Keywords: applied mechanics, applied mathematics, differential calculus, differential equations.

DOI: 10.1134/S002189442301011X

INTRODUCTION

The subject, patterns, and features of approaches in applied mathematics are considered in [1–3]. Applied mathematics uses some simplifications of the mathematical apparatus based on the classical differential calculus, i.e., the analysis of infinitesimal quantities. However, the resulting solutions describing physical processes turn out to be devoid of physical meaning.

Let us consider the classical problem of the theory of elasticity—the Flamant problem of the action of a concentrated force on a half-plane (Fig. 1). The half-plane with the Oxy coordinate system introduced therein is loaded by a concentrated force P at point O and fixed at point A to eliminate its displacement as a rigid body. This problem is considered in many monographs on the theory of elasticity, but the results of its solution are not commented on because there is no reasonable explanation to the solution obtained. Expressions for the displacements of points on the edge of the half-plane ($y = 0$, $r = x$, $\theta = \pm\pi/2$) have the following form [4]:

$$u_x(x) = \mp\frac{(1-\nu)P}{2Eh}, \qquad u_y(x) = -\frac{P}{\pi Eh}\Big(1 + \nu + 2\ln\frac{x}{y_A}\Big). \tag{1}$$

Here E and ν are the elastic modulus and Poisson's ratio of the material, h is the thickness of a plate simulated by the half-plane, and y_A is the ordinate of point A. It follows from the second equality (1) that the vertical displacement of the point where the force is applied tends to infinity, which has no physical meaning. It follows from the first equality (1) that the horizontal displacement has a discontinuity point. In this case, the boundary segments $x > 0$ and $x < 0$ are shifted as rigid bodies toward the point at which the force is applied, and the

[a]Central Research Institute for Special Machinery, Khotkovo, Russia; *vvvas@dol.ru. [b]Institute of Applied Mechanics, Russian Academy of Sciences, Moscow, Russia; salurie@mail.ru. Translated from Prikladnaya Mekhanika i Tekhnicheskaya Fizika, Vol. 64, No. 1, pp. 114–127, January–February, 2023. Original article submitted June 21, 2022; revision submitted June 21, 2022; accepted for publication September 26, 2022.

*Corresponding author.

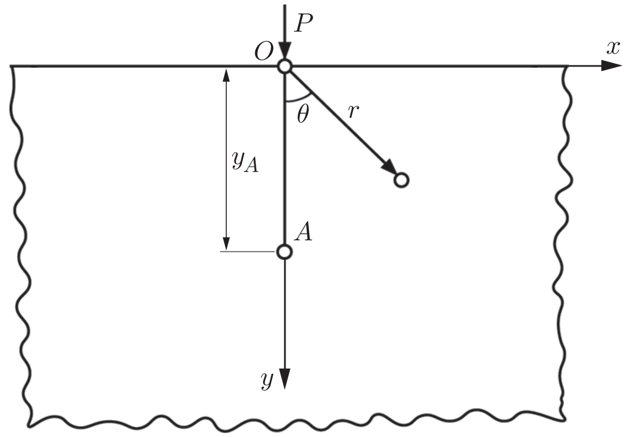

Fig. 1. Half-plane loaded with a concentrated force.

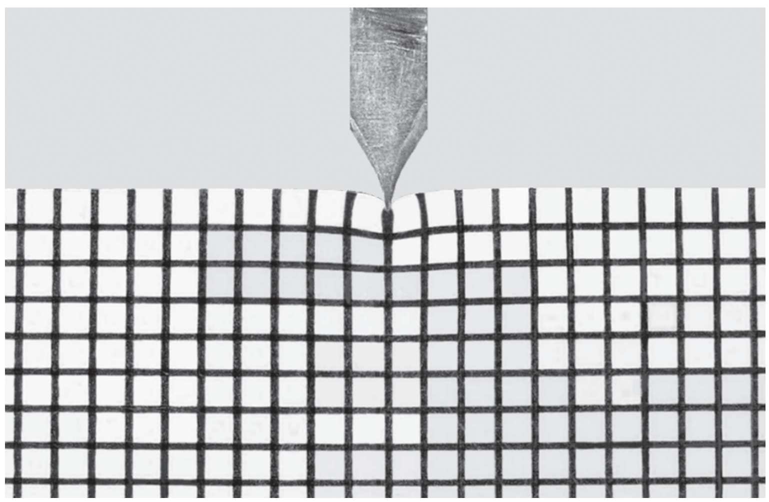

Fig. 2. Plate under local loading.

displacement has a discontinuity at the point $x = 0$. No geometric interpretation of such a displacement field is possible.

Figure 2 shows a plate made of sufficiently rigid silicone rubber ($h = 5.5$ mm, $y_A = 20$ mm, $E = 5.6$ MPa, $\nu = 0.48$, and $P = 9.8$ N [5]), loaded with a pointed indenter. A grid is applied to the plate, which makes it possible to measure displacements. In Fig. 3, the dashed curves show solution (1) and the points show the measurement results. It can be concluded that, in the experiment, displacement u_y at the point of application of the force is finite and displacement u_x, determined by the first equality (1), does not agree with the experimental data.

1. MATHEMATICAL SINGULARITY

Singular functions are fundamental solutions to the classical equations of mathematical physics. If the balance equation describing any physical process is harmonic, then the fundamental solution has a $\ln r$-type singularity for the plane problem ($r^2 = x^2 + y^2$) and a r^{-1} type singularity for the spatial problem ($r^2 = x^2 + y^2 + z^2$). In the case of a biharmonic balance equation for a plane problem, the second derivative of the fundamental solution $r^2 \ln r$ has a logarithmic singularity, while the fundamental solution to the spatial problem has a r^{-1} type singularity [6].

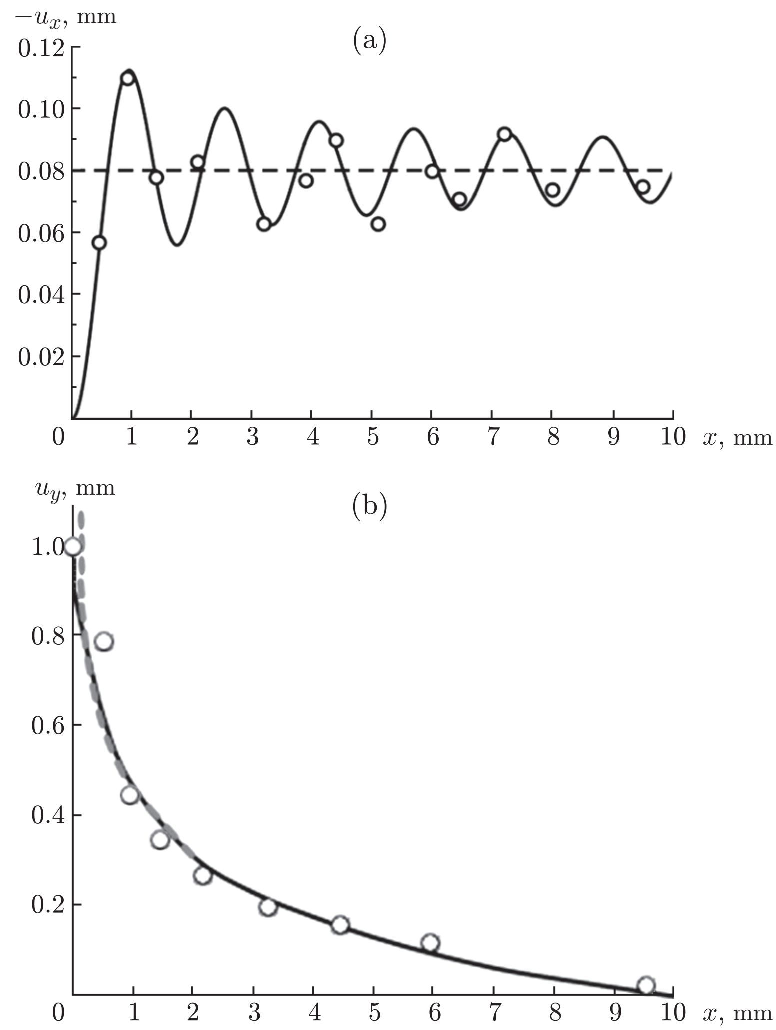

Fig. 3. Displacements $u_x(x)$ (a) and $u_y(x)$ (b) in the problem of loading a plate with a concentrated force: the solid curves refer to the generalized solution and the dashed curves to the classical solution; the points mean the experimental data.

Singularities are also derived from boundary conditions. At angular and conical points, solution singularities arise in the form of a product of power and logarithmic functions, and the exponent depends on the angle and boundary conditions. Local loading generates r^{-1} and r^{-2} type singularities in stresses for plane and spatial problems, respectively.

2. NONLOCAL FUNCTIONS

We consider the one-variable function $u(x)$ shown in Fig. 4. The traditional definition of derivative du/dx_1 assumes that the numerator and denominator of this ratio are infinitesimal. However, in problems with singular points, the numerator does not have this property. As it is known, there are discontinuities of the first kind, in which function $u(x)$ at point $x = 0$ changes by a finite value (the dashed curve in Fig. 3a), and discontinuities of the second kind, in which the function at point $x = 0$ turns to infinity (the dashed curve in Fig. 3b).

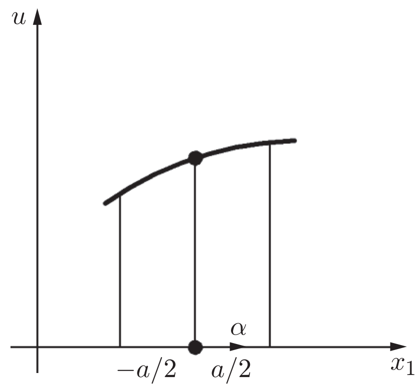

Fig. 4. One-variable function.

The singularities arising at an infinitesimal value of dx_1 are eliminated by assuming that the denominator in the derivative du/dx_1 is the finite quantity a (Fig. 4). In the vicinity of point x_1, we set a local coordinate α such that $-a/2 \leqslant \alpha \leqslant a/2$. The main idea of the proposed approach is as follows. If function $u(x_1)$ describes a real physical process, then, by definition, it is smooth and has the necessary number of derivatives with respect to x_1 at $\alpha = 0$. As function $u(x_1, \alpha)$ is expanded in a Taylor series in the vicinity of point x_1, we obtain

$$u(x_1, \alpha) = u(x_1) + \alpha u' + \frac{\alpha^2}{2!} u'' + \frac{\alpha^3}{3!} u''' + \dots \ , \tag{2}$$

where $u' = du/dx_1$. Let there be a nonlocal function $U(x_1)$ equal to the mean value of $u(x_1, \alpha)$ represented on interval $[-a/2, a/2]$ by expansion (2) [7]:

$$U(x_1) = \frac{1}{a} \int\limits_{-a/2}^{a/2} u(x_1, \alpha)\, d\alpha. \tag{3}$$

As Eq. (3) is substituted into expression (2), we obtain

$$U(x_1) = u(x_1) + \frac{a^2}{24} u''(x_1) + \dots \ . \tag{4}$$

It follows from Eq. (4) that the nonlocal function is determined at point x_1 not only by the value of the original function, but also by the values of its second derivative. A nonlocal derivative is introduced in the form of the ratio of the difference between the values of the function at the ends of the interval to the length of this interval:

$$\frac{Du}{Dx_1} = \frac{1}{a} \Big[u\Big(x_1, \frac{a}{2}\Big) - u\Big(x_1, -\frac{a}{2}\Big) \Big].$$

Substituting expansion (2) into this expression and taking into account Eq. (4), we have

$$\frac{Du}{Dx_1} = u' + \frac{a^2}{24} u''' + \dots = \frac{dU}{dx_1}.$$

Thus, the nonlocal derivative of the function is the same as the classical derivative of the nonlocal function.

3. GENERALIZED EQUATIONS

We consider an element of the medium with small but finite dimensions a, b, and c (Fig. 5). In the vicinity of point O with the x_1, x_2, and x_3 coordinates, we introduce the local coordinates α, β, and γ such that $|\alpha| \leqslant a/2$, $|\beta| \leqslant b/2$, and $|\gamma| \leqslant c/2$. Next, the symmetric tensor $t(t_1, t_2, t_3, t_{12}, t_{13}, t_{23})$ is considered, which generally describes some physical process. In special cases, this tensor can degenerate into a vector or a scalar depending on two or one variable. As above, it is assumed that the tensor components are smooth functions of the coordinates, so they are represented in the vicinity of point O as a Taylor series in the α, β, and γ coordinates:

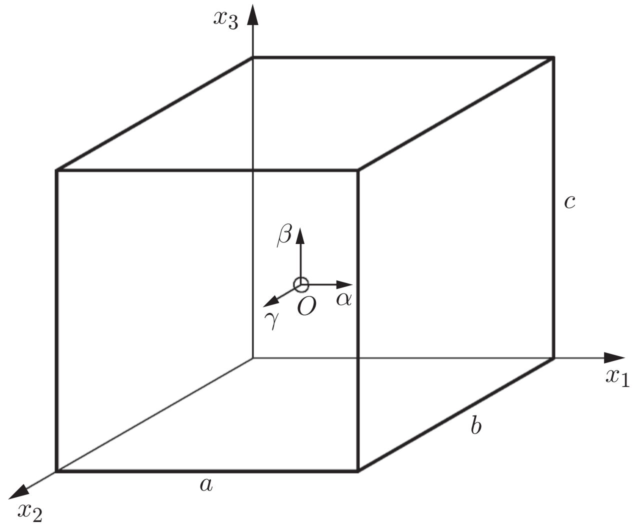

Fig. 5. Element of the medium.

$$t_{ij}(x,y,z;\alpha,\beta,\gamma) = t_{ij}(x,y,z) + \alpha t_{ij,1} + \beta t_{ij,2} + \gamma t_{ij,3} + \frac{1}{2!}\,(\alpha^2 t_{ij,11} + \beta^2 t_{ij,22} + \gamma^2 t_{ij,33}$$
$$+ 2\alpha\beta t_{ij,12} + 2\alpha\gamma t_{ij,13} + 2\beta\gamma t_{ij,23}) + \frac{1}{3!}\,(\alpha^3 t_{ij,111} + \beta^3 t_{ij,222} + \gamma^3 t_{ij,333} + 3\alpha^2\beta t_{ij,112}$$
$$+ 3\alpha\beta^2 t_{ij,122} + 3\alpha^2\gamma t_{ij,113} + 3\alpha\gamma^2 t_{ij,133} + 3\beta^2\gamma t_{ij,223} + 3\beta\gamma^2 t_{ij,233}) \qquad (5)$$

(in the subscripts, the numbers after the comma denote differentiation with respect to the corresponding coordinate). Below, we confine ourselves to the terms presented in expansion (5).

As the tensor components are averaged over the element volume similarly to Eq. (3), the following nonlocal tensor components are introduced:

$$T_{ij} = \frac{1}{abc}\int\limits_{-a/2}^{a/2}\int\limits_{-b/2}^{b/2}\int\limits_{-c/2}^{c/2} t(x_1,x_2,x_3;\alpha,\beta,\gamma)\,d\alpha\,d\beta\,d\gamma.$$

Substituting expansion (5) into this expression, we obtain

$$T_{ij} = t_{ij} + L(t_{ij})/24, \qquad L(t_{ij}) = a^2 t_{ij,11} + b^2 t_{ij,22} + c^2 t_{ij,33}. \qquad (6)$$

The equations describing the physical field are derived using the general conservation law [8], according to which the divergence of the tensor is equal to zero:

$$\frac{\partial T_{11}}{\partial x_1} + \frac{\partial T_{21}}{\partial x_2} + \frac{\partial T_{31}}{\partial x_3} = 0 \qquad (1,2,3). \qquad (7)$$

Here $(1,2,3)$ denotes a circular permutation of subscripts, which can be used to write two more equations. In the theory of elasticity, Eqs. (7) are equilibrium equations. These equations can be obtained directly from the equilibrium conditions for the element shown in Fig. 5 [9, 10]. Thus, the equilibrium equations retain their classical form, but the nonlocal tensor T_{ij} is used instead of the classical stress tensor t_{ij}. Similarly, one can obtain the equations of heat conduction and diffusion by replacing traditional variables in the corresponding classical equations with nonlocal ones. Next, the deformation of the element shown in Fig. 5 is considered. We introduce the displacement vector $u(u_1,u_2,u_3)$ and average the displacements over the faces of the selected element. In particular, the following expressions are written for faces $\alpha = \pm a/2$ and $\beta = \pm b/2$:

$$u(x,y,z;\alpha)\Big|_{\alpha=\pm a/2} = \frac{1}{bc}\int\limits_{-b/2}^{b/2}\int\limits_{-c/2}^{c/2} u(x,y,z;\alpha,\beta,\gamma)\Big|_{\alpha=\pm a/2}\,d\beta\,d\gamma,$$

$$u(x,y,z;\beta)\Big|_{\beta=\pm b/2} = \frac{1}{ac}\int\limits_{-a/2}^{a/2}\int\limits_{-c/2}^{c/2} u(x,y,z;\alpha,\beta,\gamma)|_{\beta=\pm b/2}\,d\alpha\,d\gamma.$$

The traditional approach is applied to define the linear deformations of an element with finite dimensions as the ratio of the difference between the resulting displacements of the faces to the distances between the faces and define the angular deformations as changes in the initially right angles between the coordinate planes. As a result, we have

$$E_1 = \frac{1}{a}\left[u_1(\alpha)\Big|_{\alpha=a/2} - u_1(\alpha)\Big|_{\alpha=-a/2}\right] \qquad (1,2,3),$$

$$E_{12} = \frac{1}{a}\left[u_2(\alpha)\Big|_{\alpha=a/2} - u_2(\alpha)\Big|_{\alpha=-a/2}\right] + \frac{1}{b}\left[u_1(\beta)\Big|_{\beta=b/2} - u_1(\beta)\Big|_{\beta=-b/2}\right] \qquad (1,2,3).$$

An expansion for u_i, which is similar to equality (5) for t_{ij}, is used to finally obtain

$$E_1 = \frac{\partial U_1}{\partial x_1}, \qquad E_{12} = \frac{\partial U_1}{\partial x_2} + \frac{\partial U_2}{\partial x_1} \qquad (1,2,3). \tag{8}$$

Expressions (8) coincide with the classical Cauchy relations, but include nonlocal displacements, which are expressed in terms of classical displacements by equalities similar to Eqs. (6):

$$U_i = u_i + L(u_i)/24. \tag{9}$$

Operator $L(\cdot)$ is defined by the second equality in system (6). Nonlocal displacements have a simple physical meaning: they are the displacements of the element shown in Fig. 5 averaged over the element volume. With account for the expansion for u, which is similar to Eq. (5), we have

$$\frac{1}{abc}\int\limits_{-a/2}^{a/2}\int\limits_{-b/2}^{b/2}\int\limits_{-c/2}^{c/2} u_i(x_1,x_2,x_3;\alpha,\beta,\gamma)\,d\alpha\,d\beta\,d\gamma = U_i.$$

There is a relation between nonlocal stresses and strains, which can be determined using the generalized Hooke law:

$$T_{11} = \frac{E}{1+\nu}\Big(E_{11} + \frac{\nu}{1-2\nu}\,(E_{11}+E_{22}+E_{33})\Big), \quad T_{12} = \frac{E}{2(1+\nu)}\,E_{12} \quad (1,2,3). \tag{10}$$

Relations (10) do not contradict the experimental data. As it is known, Young's modulus E and Poisson's ratio ν are determined in the experiments where the stress–strain state is uniform. In this case, operator $L(\,\cdot\,)$ included into expressions (6) and (9) for nonlocal stresses and displacements vanishes, $T_{ij} = t_{ij}$, $U_i = u_i$, and relations (10) degenerate into the classical Hooke law. It is experimentally shown in [11] that the classical Hooke law is not fulfilled at high stress gradients. Thus, the constituent relations have a classical form, but they relate nonlocal functions. It can be assumed for an isotropic body that $b = c = a$. Then, Eqs. (6) and (9) take the form

$$T_{ij} = t_{ij} + \frac{a^2}{24}\,\Delta(t_{ij}), \qquad U_i = u_i + \frac{a^2}{24}\,\Delta(u_i), \tag{11}$$

where Δ is the three-dimensional Laplace operator. For two-dimensional problems, we have $b = a$, $c = 0$, while Δ is a two-dimensional Laplace operator. For one-dimensional problems, $b = c = 0$ and $\Delta(\cdot) = d^2(\cdot)/dx_1^2$. If the argument is a scalar function, then the Laplace operator is invariant and relations similar to (11) are valid in any coordinate system.

The main idea of the proposed approach is as follows. As follows from the above, the proposed generalized field equations coincide with the classical equations, but they include nonlocal functions instead of traditional functions. Thus, if a classical solution is obtained, then the corresponding nonlocal functions are also known. The classical variables are obtained by integrating the system of Helmholtz equations (11). The known nonlocal functions are substituted into the left parts of these equations. The general solution to the Helmholtz equations consists of a particular solution and a general solution to the corresponding homogeneous equation. If, in addition, the traditional solution has singular points, then the particular solution has this property too, and, with an appropriate choice of integration constants, the general solution makes it possible to eliminate the singularities of the particular solution and obtain a regular solution. It should be noted that this is possible if a physical process is considered. If some abstract functions with singular points are substituted into the left parts of Eqs. (11), then the solution to the homogeneous Helmholtz equation prevents from eliminating them. Thus, the proposed approach is not universal as it is applicable only to applied problems. Some applications of the proposed approach are considered below.

4. APPLICATION OF THE METHOD TO PROBLEMS OF THE THEORY OF ELASTICITY

Two problems are under study.

Problem 1. There is a circular membrane fixed along a contour with radius R and loaded at the center with a concentrated force P and line forces t that create its pretension (a classical singular problem of mathematical physics [12]). The membrane deflection satisfies the equation

$$t\,\Delta w = -p(r), \qquad \Delta(w) = \frac{1}{r}\frac{d}{dr}(rw'). \tag{12}$$

Here $0 \leqslant r \leqslant R$ is the radial coordinate and $(\cdot)' = d(\cdot)/dr$. For a membrane loaded at the center with a concentrated force, pressure $p(r)$ can be expressed in terms of the delta function, i.e., $p(r) = P\delta(r)$. A solution to Eq. (12), which satisfies the condition of fixing the membrane $w(r)\Big|_{r=R} = 0$, has the form [12]

$$w = \frac{P}{2\pi t}\ln\frac{R}{r}. \tag{13}$$

Hence $w \to \infty$ as $r \to 0$. It is noteworthy that deflection turns to infinity for any value of force P, no matter how small it is. Solution (13) to Eq. (12) has a fundamental drawback of the classical formulation of the problem. The right side of Eq. (12) is singular, and solution (13) is also singular. From the point of view of mathematics, this solution is correct because a singular action causes a singular reaction. However, when solving an applied problem, such a result is unacceptable as the concepts of force P and deflection w are fundamentally different. The concentrated force does not exist in reality and is the limit of product of pressure and the area of the site on which it acts if the pressure tends to infinity and the area of the site tends to zero. As noted above, it is impossible to eliminate such a singularity because it is introduced by definition. However, deflection is a physical quantity that can be measured and cannot be infinitely large. Note that mathematics has a proof of correctness of solution (13), which is represented as a limit function of a sequence of regular solutions [13]. However, the obtained result has no physical meaning. Thus, the mathematical correctness of the solution does not ensure its physical reliability.

It is noteworthy that integration lowers the order of the singularity. Therefore, it can be assumed that the order of Eq. (11) is insufficient to obtain a physically correct solution. In the proposed approach, there is an increase in the order due to the Helmholtz equation (11), which for the problem under consideration has the following form:

$$W = w + \frac{a^2}{24}\Delta(w). \tag{14}$$

Because the deflection is a scalar function, the Laplace operator has the property of invariance, is written in polar coordinates, and is determined by the second equality (12). The classical solution (13) should be substituted into the left side of Eq. (14). As a result, we have

$$\frac{a^2}{24}\Delta(w) + w = \frac{P}{2\pi t}\ln\frac{R}{r}. \tag{15}$$

Next, parameter a, included in Eq. (15), is to be determined. In order to do this, a problem in a space with a large number of dimensions is considered, i.e., a membrane not seen as a two-dimensional mathematical manifold, but as a three-dimensional object having a thickness. Then the membrane can be interpreted as a circular plate of finite thickness h. The equation describing the deflection of a circular plate loaded at the center with a concentrated force has the form [14]

$$-\frac{D}{t}\Delta(w) + w = \frac{P}{2\pi t}\ln\frac{R}{r}, \tag{16}$$

where $D = Eh^3/[12(1-\nu^2)]$ is the bending stiffness of the plate. It can be concluded from comparing Eqs. (15) and (16) that $a^2 = -24D/t$. Because D and t cannot be negative, a is imaginary. This result seems natural because the proposed theory is phenomenological: it is based on the continuum model of the medium that does not take into account its real microstructure. Therefore, within the framework of such a model, it is impossible to obtain information about the structure of the medium, particularly about the actual dimensions of the element shown in Fig. 5.

Let there be a real parameter $s^2 = -a^2/24$. Then, Eqs. (11) take the final form

$$T_{ij} = t_{ij} - s^2\,\Delta(t_{ij}), \qquad U_i = u_i - s^2\,\Delta(u_i). \tag{17}$$

Equation (15) is rewritten as [15]

$$\frac{d^2w}{d\rho^2} + \frac{1}{\rho}\,\frac{dw}{d\rho} - w = -\frac{P}{2\pi t}\ln\frac{R_s}{\rho}, \quad \rho = \frac{r}{s}, \quad R_s = \frac{R}{s}. \tag{18}$$

The general solution to the homogeneous equation that corresponds to Eq. (18) is expressed in terms of the modified Bessel functions $I_0(\rho)$ and $K_0(\rho)$ and the corresponding particular solution. It is noteworthy that, as the right side of Eq. (18) satisfies the Laplace equation, it is a particular solution to this equation. Finally, we have

$$w(\rho) = C_1 I_0(\rho) + C_2 K_0(\rho) + \frac{P}{2\pi t}\ln\frac{R_s}{\rho}. \tag{19}$$

The constant C_1 is determined from the boundary condition $w(\rho)\Big|_{\rho=R_s} = 0$, thereby obtaining

$$w(\rho) = C_2\Big(K_0(\rho) - \frac{K_0(R_s)}{I_0(R_s)}\,I_0(\rho)\Big) + \frac{P}{2\pi t}\ln\frac{R_s}{\rho}. \tag{20}$$

Note that, in addition to the last term, which increases indefinitely as $\rho \to 0$, the solution includes the Macdonald function $K_0(\rho)$, which also turns to infinity for $\rho = 0$. Thus, it is possible to eliminate the singularity of solution (20) by choosing constant C_2. It is carried out by expanding the Bessel functions into power series of the form [16]

$$I_0(\rho) = 1 + \frac{\rho^2}{4(1!)^2} + \frac{\rho^4}{4^2(2!)^2} + \ldots, \qquad K_0(\rho) = -\Big(\gamma + \ln\frac{\rho}{2}\Big)I_0(\rho) + \frac{\rho^2}{4(1!)^2} + \ldots, \tag{21}$$

where $\gamma = 0.577$ is Euler's constant. Substituting series (21) into solution (20) and passing to the limit as $\rho \to 0$, we can conclude that the deflection at the center of the plate is finite if $C_2 = -P/(2\pi t)$. Finally, it is written that

$$w(\rho) = \frac{P}{2\pi t}\Big(\ln\frac{R_s}{\rho} - K_0(\rho) + \frac{K_0(R_s)}{I_0(R_s)}\,I_0(\rho)\Big). \tag{22}$$

The derivative of the deflection

$$w' = \frac{1}{s}\,\frac{dw}{d\rho} = \frac{P}{2\pi t s}\Big(K_1(\rho) - \frac{1}{\rho} + \frac{K_0(R_s)}{I_0(R_s)}\,I_1(\rho)\Big)$$

at the center of the membrane turns to zero because $K_1\Big|_{\rho\to 0} \to 1/\rho$, $I_1(0) = 0$.

The resulting solution was verified in the experiments [15] with a 0.04-mm thick membrane made of a polymer film with aluminum coating and the material constants $E = 5.4$ GPa and $\nu = 0.4$. A pretension $t = 0.77$ N/mm was created in the membrane. Calculation resulted in $s = 0.216$ mm. Figure 6 shows the deflection distribution along the membrane radius at a force $P = 0.5$ N. The solid curve corresponds to solution (22), and the points show the experimental data. The difference between the generalized and classical solutions is manifested only near the center of the membrane. The computational results are shown in Fig. 7, where the dashed curve corresponds to solution (13) and the solid curve to solution (22).

It should be noted that a regular solution to Eq. (18) with a logarithmic singularity does not exist if an arbitrary singularity is introduced into the right side of the equation. As noted above, the proposed approach is not universal and the singularity is eliminated in problems having a physical meaning.

Problem 2. We consider the problem of the theory of elasticity about a plate with a central crack under tension (Fig. 8). For $x \geqslant c$ and $\theta = 0$, an expression for stress σ_y has the following form [17]:

$$\sigma_y = \frac{\sigma x}{\sqrt{x^2 - c^2}}. \tag{23}$$

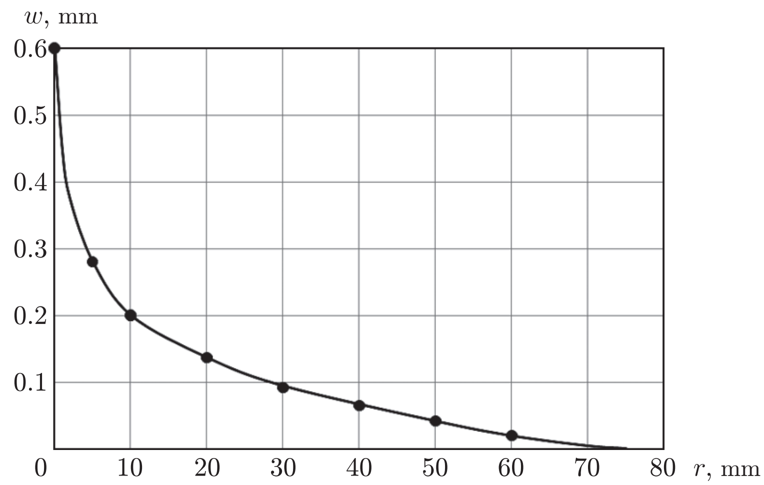

Fig. 6. Deflection distribution over the membrane radius: the solid curve shows solution (22) and points refer to the experimental data.

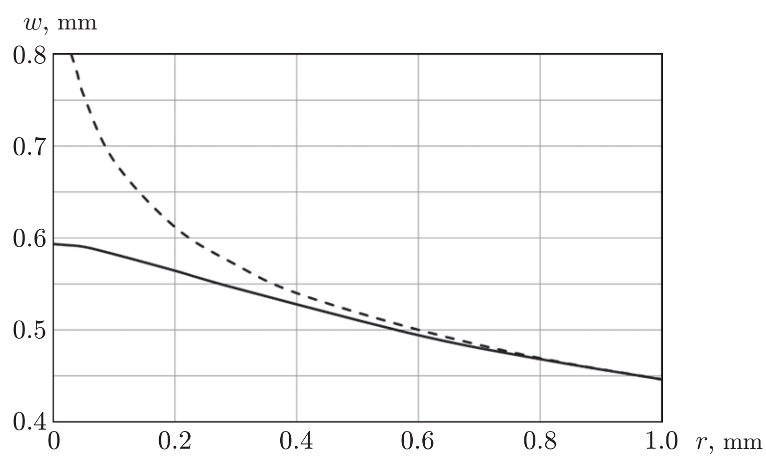

Fig. 7. Deflection in the vicinity of the center of the membrane: the dashed curve refers to the classical solution and the solid curve to the generalized solution.

Consequently, the stress at the crack tip is infinitely large for the arbitrarily small acting stress σ. This means that the brittle material plate, whose strength is determined by the maximum stress, does not take the load. This contradicts the experimental results, according to which the cracked brittle material plates have a certain load-bearing capacity. The generalized solution to the problem presented in [18] makes it possible to obtain the following expression for the stress:

$$\frac{\sigma_y}{\sigma} = \frac{1}{\sqrt{\bar r}}\Big[\frac{1+\bar r}{\sqrt{2+\bar r}} - \frac{1}{8\sqrt{2}}\Big(2+\frac{3}{\lambda}+\frac{15}{8\lambda^2}\Big)\,\mathrm{e}^{-\lambda\bar r}\Big] + \frac{3}{8\lambda\sqrt{2\bar r^3}}\Big(4-\frac{1}{\lambda}\Big)\,\mathrm{e}^{-\lambda\bar r}$$
$$- \frac{6}{\lambda^2\sqrt{\bar r^5}}\Big(\frac{1+\bar r}{\sqrt{(2+\bar r)^5}} - \frac{1}{4\sqrt{2}}\,\mathrm{e}^{-\lambda\bar r}\Big), \quad x \geqslant c, \quad \theta = 0. \tag{24}$$

Here $\lambda = c/s$ and $\bar r = r/c$ (r is the distance from the crack end measured along the x axis). The dependences of the stress on the dimensionless distance $\bar r$ for different values of λ are shown as solid curves in Fig. 9. The dashed curve corresponds to the classical solution (23). It follows from Fig. 9 that the maximum stresses are finite. Let the maximum stress be denoted by $\sigma_m(\lambda)$ and divided by stress σ acting on the plate (Fig. 8), thereby obtaining the stress concentration factor $k_\sigma = \sigma_m(\lambda)/\sigma$. The dependence of k_σ on λ, constructed using solution (24), is shown in Fig. 10. This dependence is valid for plates of any material.

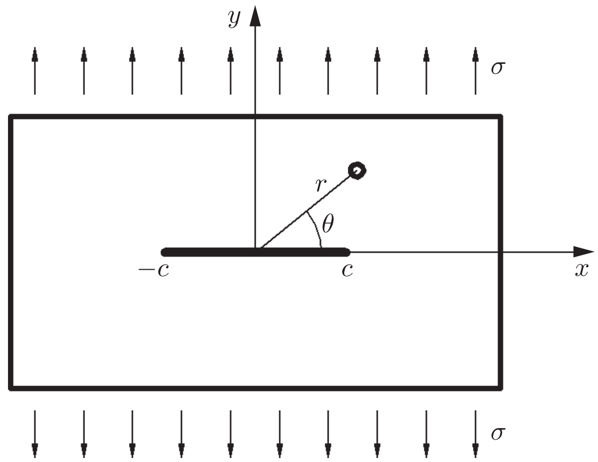

Fig. 8. Tension of the plate with a crack.

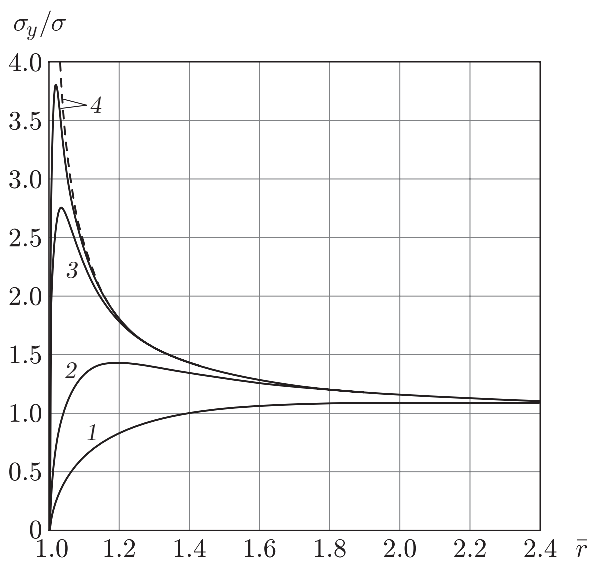

Fig. 9. Dependences $\sigma_y(\bar{r})$ for $\lambda = 3$ (*1*), 10 (*2*), 50 (*3*), and 100 (*4*): the solid curves refer to the solution (24) and the dashed curve refers to the classical solution (23).

Determining $\lambda = c/s$ requires that s is obtained, which is included in the Helmholtz equations (17). As it is impossible to determine this parameter analytically using a more general model of the plate, it is proposed to obtain it experimentally. For this purpose, a polymethyl methacrylate (Plexiglas) plate is tested for tension, which is a brittle material with a tensile strength $\bar{\sigma} = 83.3$ MPa, determined with an accuracy of 1.3%. A 99-mm wide and 2.93-mm thick plate has a central crack with a length $c = 10.8$ mm. The plate collapses under a stress $\sigma = 7.06$ MPa. Thus, the stress concentration factor in the experiment is $k_\sigma = \bar{\sigma}/\sigma = 11.8$. The dependence shown in Fig. 10 is used to obtain $\lambda = 1000$. Then, $s = c/\lambda = 0.0108$ mm. Because s is determined experimentally, the question arises about the degree of its invariance, i.e., about the possibility of predicting the bearing capacity of plates of a similar material with cracks of other sizes. A plate with a crack of a size $c = 6$ mm collapses at a stress $\sigma = 9.36$ MPa. For $s = 0.0108$ mm, we have $\lambda = c/s = 556$; using the dependence shown in Fig. 10, we obtain $k_\sigma = 8.9$ and the stress limit value $\sigma = 9.36$ MPa, which coincides with the experimental value. A plate with a crack $c = 18$ mm collapses at a stress $\sigma = 5.35$ MPa. The values obtained in the calculation are $\lambda = 1667$,

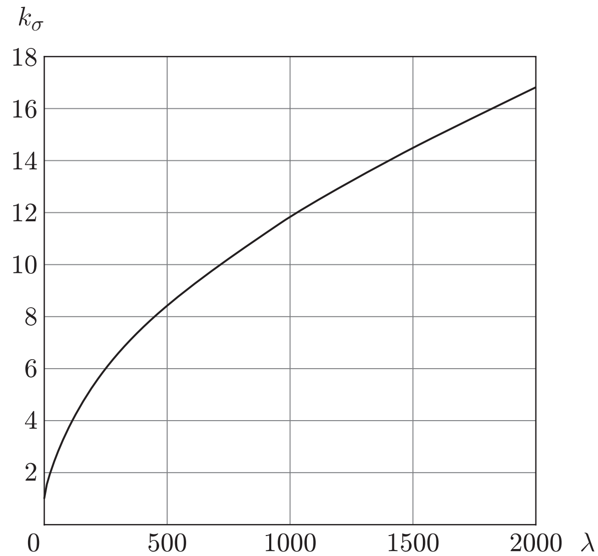

Fig. 10. Stress concentration factor k_σ versus λ.

$k_\sigma = 15.5$, and $\sigma = 5.37$ MPa, which differs from the experimental value by 0.4%. Thus, the value of s obtained in one of the experiments makes it possible to calculate the critical stress for plates with cracks of various lengths. Moreover, it is experimentally shown that s obtained in the tension of the plate with a central crack can be used to estimate the strength of tensile and bent plates with lateral cracks [18].

As for the Flamant problem considered in Introduction, the generalized solution to this problem given in [5] suggests the following expressions for the displacements of the half-plane boundary $\theta = \pm\pi/2$ (Fig. 1):

$$u_x(x) = \mp\frac{(1-\nu)P}{2Eh}\left[1 - J_0\left(\frac{x}{s}\right)\right],$$

$$u_y(z) = \frac{2P}{\pi Eh}\left[K_0\left(\frac{y_A}{s}\right) - K_0\left(\frac{x}{s}\right) + \ln\left(\frac{y_A}{x}\right)\right] + \frac{(1+\nu)P}{\pi Eh}\left[K_2\left(\frac{x}{s}\right) - K_2\left(\frac{y_A}{s}\right) + \frac{2s^2}{y_A^2} - \frac{2s^2}{x^2}\right].$$

For a silicone rubber plate (Fig. 2), the value $s = 0.25$ mm is experimentally obtained. The calculated dependences for the displacements $u_x(x)$ and $u_y(x)$ are shown by the solid curves in Fig. 3 and are in good agreement with the experimental data.

5. MATHEMATICAL SINGULARITIES AND REALITY

As noted above, there are singular functions in solutions to problems of mathematical physics if these problems are considered in the classical formulation. The results obtained are usually interpreted via the traditional approach, according to which the solution is considered as reliable at all points, except for the region in the vicinity of the singularity point. At the same time, the question of the size of this region remains open, but on the whole the validity of the singular solution is not questioned. However, this approach is not used in mathematical works stating that the mathematical singularity is real. In particular, we consider the mathematical problem of the singularity of solutions to algebraic equations describing curves with kinks and self-intersections. An example of such a curve is a signature that includes similar points at which, as stated in [19], singularities are formed. This does not take into account that, unlike a one-dimensional manifold, which is a mathematical model of a curve, the signature is a three-dimensional object whose width and thickness are small but finite. At the points of intersection, the lines are located at different levels, there are no curve self-intersections and no singularity. Even more categorical is the statement that singularities exist everywhere in the real world [20]. In particular, singularity appears at the fold of a newspaper as the curvature goes to infinity. This does not take into account that a newspaper sheet is not a two-dimensional manifold, but has a finite thickness and bending stiffness. The bending of a newspaper is described by the theory of plates, from which it follows that an infinitely large curvature can be formed only as a result of applying an infinitely large bending moment, which is physically unrealistic. Thus, the existence of a mathematical singularity is based on the transfer of formal mathematical results obtained using computational models that are inadequate from the point of view of physics.

CONCLUSIONS

It is suggested that singular and discontinuous solutions should be considered as formal mathematical results with no physical meaning. Physical processes may be described using the generalized statement of the problem, which includes, along with traditional equations, the Helmholtz equations containing an additional experimental constant and allowing one to obtain regular solutions.

This work was financially supported by Grant No. 075-15-2022-1023.

REFERENCES

1. I. I. Blekhman, A. D. Myshkis, and Ya. G. Panovko, *Applied Mathematics: Subject, Logic, and Approaches* (Naukova Dumka, Kiev, 1976) [in Russian].
2. I. I. Blekhman, A. D. Myshkis, and Ya. G. Panovko, *Mechanics and Applied Mathematics. Logic and the Application of Mathematics* (Nauka, Moscow, 1990) [in Russian].
3. I. I. Blekhman, A. D. Myshkis, and Ya. G. Panovko, *Applied Mathematics: Subject, Logic, and Approaches* (Naukova Dumka, Kiev, 2018) [in Russian].
4. S. P. Timoshenko and J. N. Goodier, *Theory of Elasticity* (McGraw-Hill Book Company, Inc., 1951).
5. V. V. Vasiliev, S. A. Lurie, and V. A. Salov, "On the Flamant Problem for a Half-Plane Loaded with a Concentrated Force," Acta Mech. **232** (4), 1–11 (2021).
6. A. D. Polyanin, *Handbook of Linear Equations of Mathematical Physics* (Fizmatlit, Moscow, 2001) [in Russian].
7. V. V. Vasiliev and S. A. Lurie, "Nonlocal Solutions to Singular Problems of Mathematical Physics and Mechanics," Prikl. Mat. Mekh. **18** (2), 459–471 (2018) [Mech. Solids **53**(2), 135–144 (2018); DOI: https://doi.org/10.3103/S0025654418050163].
8. J. L. Synge, *Relativity: The General Theory* (North-Holland Publ. Comp., Amsterdam, 1930).
9. V. V. Vasiliev and S. A. Lurie, "Generalized Theory of Elasticity," Izv. Ross. Akad. Nauk, Mekh. Tv. Tela, No. 4, 16–27 (2015).
10. V. V. Vasiliev and S. A. Lurie, "A New Solution to the Axisymmetric Contact Problem in the Theory of Elasticity," Izv. Ross. Akad. Nauk, Mekh. Tv. Tela, No. 5, 12–21 (2017).
11. A. V. Andreev, *Engineering Methods for Determining Stress Concentration in Machine Parts* (Mashinostroenie, Moscow, 1976) [in Russian].
12. S. G. Mikhlin, *Linear Equations in Partial Derivatives* (Vysshaya Shkola, Moscow, 1977) [in Russian].
13. S. L. Sobolev, *Equations of Mathematical Physics* (Gostekhteoretizdat, Moscow–Leningrad, 1950) [in Russian].
14. Tsan Vei-Chan (Ed.), *Theory of Flexible Circular Plates* (Izd. Inostr. Lit., 1967) [in Russian].
15. V. V. Vasiliev and S. A. Lurie, "Generalized Solution to the Problem of a Circular Membrane Loaded with a Concentrated Force," Izv. Ross. Akad. Nauk, Mekh. Tv. Tela, No. 3, 115–119 (2016).
16. *Handbook on Special Functions with Formulas, Graphs, and Mathematical Tables* (Nauka, Moscow, 1968) [in Russian].
17. Yu. N. Rabotnov, *Mechanics of a Deformable Solid* (Nauka, Moscow, 1979) [in Russian].
18. V. V. Vasiliev, S. A. Lurie, and V. A. Salov, "Estimation of the Strength of Plates with Cracks Based on the Maximum Stress Criterion in a Scale-Dependent Generalized Theory of Elasticity," Fiz. Mezomekh. **21** (4), 5–12 (2018) [Phys. Mesomech. **22**, 456–462 (2019); DOI: https://doi.org/10.1134/S102995991906002X].
19. "Interview with Heisuka Hironaka," Notices AMS **52** (9), 1010–1019 (2005).
20. Sh.-T. Yau and S. Nadis, *The Shape of Inner Space: String Theory and the Geometry of the Universe's Hidden Dimensions* (Il Saggiatore, 2010).